

Open Research Online

The Open University's repository of research publications and other research outputs

Design and characterisation of the new CIS115 sensor for JANUS, the high resolution camera on JUICE

Conference or Workshop Item

How to cite:

Soman, Matthew; Holland, Andrew; Stefanov, Konstantin; Gow, Jason; Leese, Mark; Pralong, Jérôme and Turner, Peter (2014). Design and characterisation of the new CIS115 sensor for JANUS, the high resolution camera on JUICE. In: High Energy, Optical, and Infrared Detectors for Astronomy VI, article no. 915407.

For guidance on citations see [FAQs](#).

© 2014 Society of Photo-Optical Instrumentation Engineers

Version: Accepted Manuscript

Link(s) to article on publisher's website:
<http://dx.doi.org/doi:10.1117/12.2056810>

Copyright and Moral Rights for the articles on this site are retained by the individual authors and/or other copyright owners. For more information on Open Research Online's data [policy](#) on reuse of materials please consult the policies page.

oro.open.ac.uk

Design and characterisation of the new CIS115 sensor for JANUS, the high resolution camera on JUICE

Matthew Soman^a, Andrew D. Holland^a, Konstantin D. Stefanov^a, Jason P. Gow^a, Mark Leese^a, Jérôme Pratlong^b, Peter Turner^b

^aCentre for Electronic Imaging, The Open University, MK7 6AA, UK.

^be2v technologies plc., 106 Waterhouse Lane, Chelmsford, Essex, CM1 2QU, UK.

ABSTRACT

JUICE, the Jupiter Icy Moon Explorer, is a European Space Agency L-class mission destined for the Jovian system. Due for launch in 2022, it will begin a science phase after its transit to Jupiter that will include detailed investigations of three of the Galilean moons: Ganymede, Callisto and Europa. JUICE will carry payloads to characterise the Jovian environments, divided into in situ, geophysical and remote sensing packages.

A key instrument in the remote sensing package is JANUS, an optical camera operating over a wavelength range of 350 nm to 1064 nm. JANUS will be used to study the external layers of Jupiter's atmosphere, the ring system and the planetary bodies. To achieve the science goals, resolutions of better than 5 m per pixel are required for the highest resolution observations during the 200 km altitude orbit of Ganymede, whilst the system is operated with a signal to noise ratio of better than 100.

Jupiter's magnetic field is a dominant object in the solar system, trapping electrons and other charged particles leading to the radiation environment around Jupiter being very hostile, especially in the regions closest to Jupiter in the Ganymede orbit. The radiation tolerance of the focal plane detector in JANUS is therefore a major concern and radiation testing is vital to confirm its expected performance after irradiation will meet requirements set by the science goals.

JANUS will be using a detector from e2v technologies plc, the CMOS Imaging Sensor 115 (CIS115), which is a device manufactured using 0.18 um Imaging CMOS Process with a 2000 by 1504 pixel array each 7 um square. The pixels have a 4T pinned photodiode pixel architecture, and the array is read out through four differential analogue outputs. This paper describes the preliminary characterisation of the CIS115, and results obtained with the CIS107 precursor sensor.

Keywords: JUICE, JANUS, CIS107, CIS115, CMOS, APS.

1. INTRODUCTION

The JUUpiter ICy moons Explorer (JUICE) is a European Space Agency (ESA) Large-class mission with a launch date planned for 2022 [1][2]. The spacecraft will enter a cruise phase until arrival in the Jovian system in 2030, where its scientific payload will perform detailed remote and in-situ characterisation of Jupiter and its natural satellites. Specific mission phases are planned for spacecraft orbit around the three of the Galilean satellites: Callisto, Ganymede and Europa, where the on-board high resolution camera will perform detailed mapping of the surface terrain at multiple wavelengths.

The camera, named JANUS (Jovis, Amorum ac Natorum Undique Scrutator) [3], uses a Three Mirror Anastigmat optical design from ROSETTA heritage [4] with an entrance pupil diameter of 100 mm and overall field of view of 1.72×1.29 degrees² on the CMOS sensor. The wide angle will be aligned perpendicular to the direction of motion of the spacecraft to maximize the swath width during flybys. A 14-space filterwheel provides spectral analysis capability across the sensor's sensitive wavelength range by incorporating narrow and broad band filters from 350 nm to 1064 nm.

*matthew.soman@open.ac.uk; www.open.ac.uk/cei

2. JANUS SENSOR

2.1 CIS115 Sensor

The CIS115 is the next generation CMOS Imaging Sensor developed by e2v technologies plc (e2v) [5] that is baselined as the imaging sensor for JANUS. It has been developed following an in-depth investigation into its predecessor device, the CIS107 (Figure 1). The CIS107 has the same form factor as the CIS115 but its imaging area is subdivided into 10 different pixel layouts, 6 metalisation variants and 3 types of output driver to compare and assess the performance of each combination. Both front and back-illuminated CIS107s were manufactured on standard and high resistivity silicon, and they underwent detailed electro-optic characterisation, proton and gamma irradiation campaigns. Following these studies, a single pixel variant and output type was taken forward to the CIS115, with minor modifications made to further improve its performance.

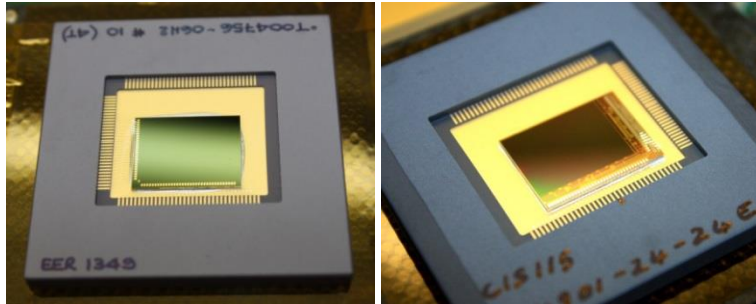


Figure 1. The back-illuminated CIS107 (left) is a predecessor test device, and the front-illuminated CIS115 (right) is the first CIS115 variant that has become available for testing. The devices are connected to their packages on two sides of the die, making the sensors two-side buttable for future applications.

The CIS107 and CIS115 are manufactured using the Tower 018 Imaging Sensor process, with a 2000×1504 pixel region that is divided into 4 areas (each 2000 rows by 376 columns), see Figure 2. Each quarter of the imaging area has its own analogue output capable of sampling up to 10 MPixel second⁻¹. The pixels contain rectangular pinned photodiodes with 4T pixel architecture, arranged with a pitch of $7 \mu\text{m}$.

The CIS115 sensor for JANUS will be optimized for sensitivity by thinning the epitaxial silicon to approximately $10 \mu\text{m}$ and being back-illuminated to result in a 100% fill factor. A wide-band anti-reflection coating will be applied providing expected Quantum Efficiency (QE) better than 70% at wavelengths from 400 nm to 750 nm at -40°C (Figure 3). The sensor is manufactured using high resistivity epitaxial silicon (approximately $1000 \Omega \text{cm}$) to increase the depth of depletion of the photo-diodes, improving the spatial resolution. The sensor will be cooled using a cold finger leading to a radiator external to the spacecraft, with an operational temperature of $-50 \pm 5^\circ\text{C}$ currently specified to reduce the contribution of dark signal to the background noise.

2.2 Sensor readout procedure

The 4T pixel architecture allows the sensors to be operated in a rolling shutter mode where the output node is sampled after reset and after transfer of the signal from the photodiode. The readout occurs simultaneously in each of the four image areas. First the reset levels of every pixel in the row currently selected (4×376 pixels) are transferred to a set of storage capacitors in the 'CDS buffer' (Figure 4). The charges from the row's photodiodes are then simultaneously transferred and also stored in the CDS buffer. The time at which integration begins and ends is therefore the same for all pixels in a row and the rolling shutter occurs in a row by row fashion. The process of transferring the reset and signal levels of a row into the CDS buffer has a duration of t_{CDS} , typically $10 \mu\text{s}$.

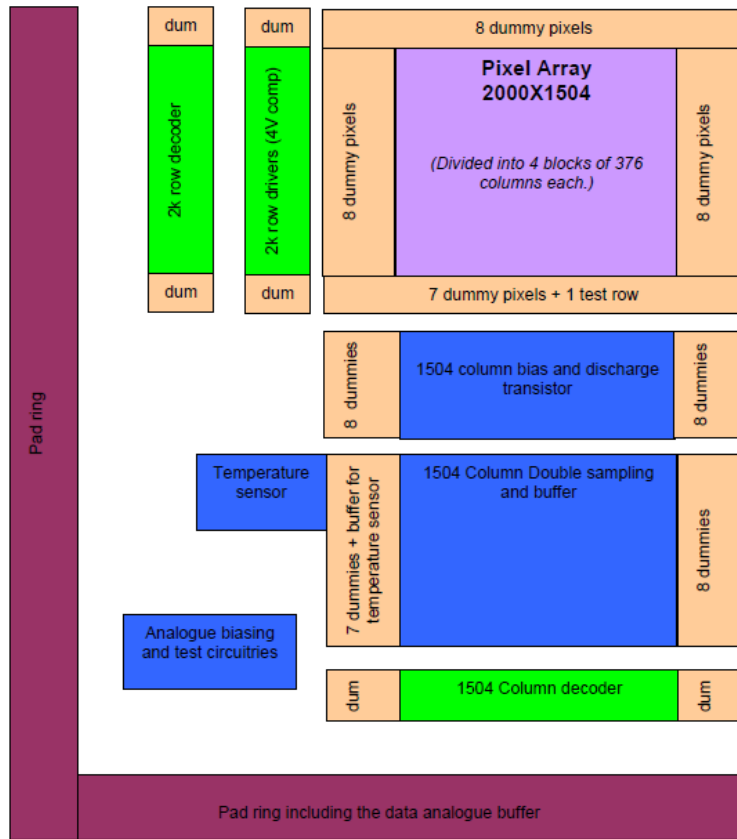


Figure 2. Block diagram of the CIS115 sensor showing the image area divided into four sections, with four parallel outputs. The CIS107 has an identical architecture but the 10 pixel design variants were used in the image area, each with 6 metalisations, and there were three different types of output.

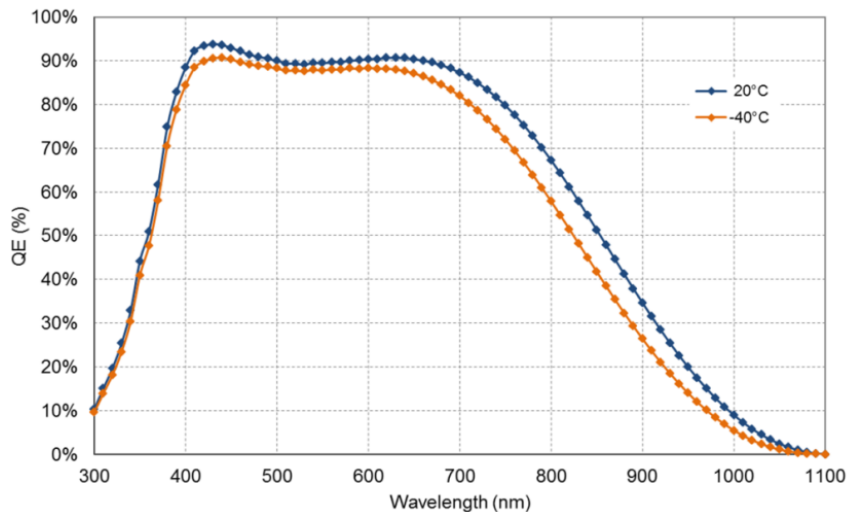


Figure 3. The predicted QE performance of the back-illuminated CIS115 when coated using e2v's Multilayer-2 anti-reflective coating is better than 70% at wavelengths from 400 nm to 750 nm at -40°C. The QE degrades at longer wavelengths where silicon becomes more transparent due to the sensitive silicon thickness being approximately 10 μm thick.

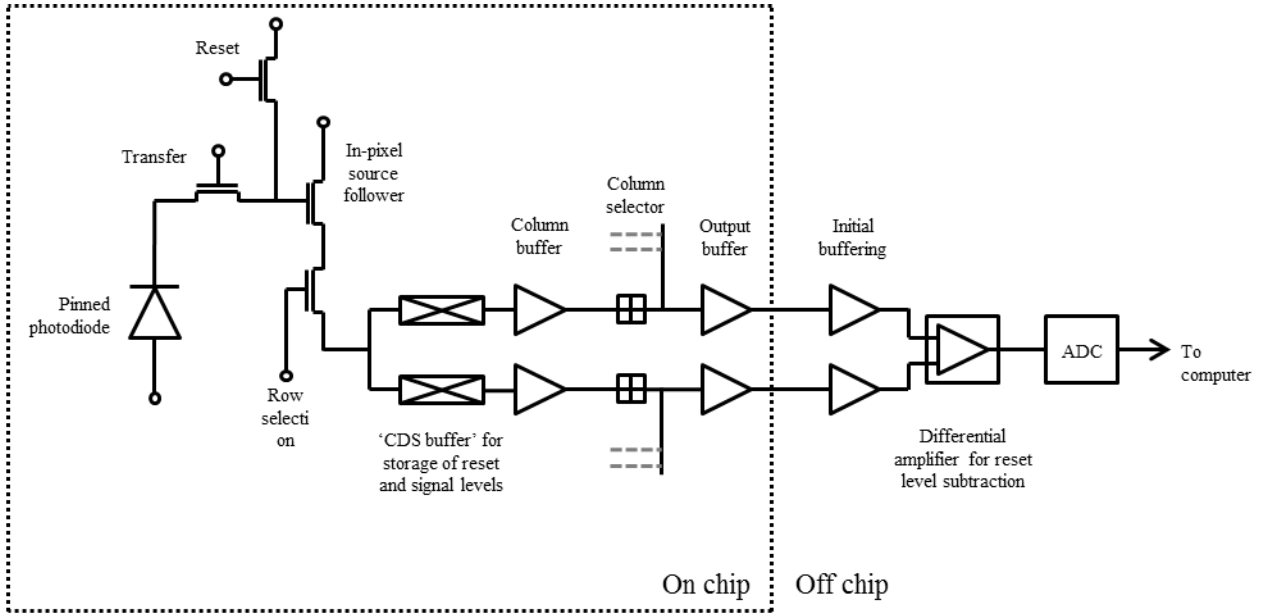


Figure 4. The readout pathway for a single pixel is shown for the CIS107/CIS115 and off-chip camera setup, as described in the text. The CIS115 output has a limited drive capacity (<6 pF), therefore buffer amplification is required close to the output pins.

The stored signal and reset values are transferred off the die through four pairs of pins – a reset and signal pin per analogue output. When a column (1 to 376) is selected, the reset and signal levels of the four pixels with that column address are presented simultaneously on the output pins. The output nodes are capable of readout rates, r_r , of up to 10 MHz per output and so the total readout time, t_{total} , for an image with N_r rows and N_c columns is given by equation 1.

$$t_{total} = \left(\frac{N_c}{r_r} + t_{CDS} \right) N_r \quad (1)$$

In full frame readout mode, with $t_{CDS} = 10 \mu\text{s}$ and a pixel sample rate of 5 MHz, the total readout time is 170.4 ms. When N_r is large, as it is in the full frame case, the integration time is approximately equal to t_{total} . Increasing the integration time can be achieved by adding the appropriate pause between frames, however shorter integration times will also be required for JANUS as the image dwell time is expected to be 4 ms during the spacecraft's 400 km orbit of Ganymede. To achieve integration times shorter than the readout time, a row of photodiodes may be reset at the arbitrary time before it is read out. This additional reset process may occur when a different row is being read out from the CDS buffer, preventing it extending the readout time. When an extremely short integration time is required ($\ll 1$ ms), for example to measure pixel noise with minimal dark current contribution, a row may be reset immediately before it is sampled into the CDS buffer.

2.3 Device status

The first wafers of back-illuminated CIS115s are expected to be manufactured by September 2014, however the first front-illuminated CIS115s have been packaged and are undergoing preliminary characterisation. The pin-out and operation of CIS107s is identical to the CIS115s, therefore back-illuminated CIS107s have been used to verify the experimental setup and commission the test camera. Results from the relevant pixel variant of the CIS107 are indicative of the performance to be expected from the CIS115s; therefore measurements are presented alongside CIS115 results in Table 1 and the following sections.

Parameter	Units	CIS107: pixel variant 1	CIS115	
		Measured	Goal	Measured
Columns	pixels	1504		
Rows	pixels	2000		
Pixel pitch	μm	7		
Image area	mm	10.528×14.000		
Outputs	-	4		
Maximum output	V	1.8		
Readout rate	MPixel s^{-1} output $^{-1}$	≤ 10		
Responsivity	$\mu\text{V electron}^{-1}$	34.1	45	48.3
Readout Noise (at 5 MPixel s^{-1} output $^{-1}$)	electrons rms	5.6	<8	4.25
Full well capacity	electrons	55k	39k	-
Dark current (21°C)	electrons pixel $^{-1}$ s $^{-1}$	51	30	22
Radiation performance	krad (Si)	Measured up to 150	>200	TBM
	protons cm^{-2}	Measured at 2×10^{10} (58.8 MeV)	$>2 \times 10^{10}$ (10 MeV equivalent)	TBM

Table 1. Parameters of the CIS107 and CIS115 that have been measured or are inferred by design. TBM: To Be Measured.

Once the back-illuminated CIS115s have been characterised, irradiation campaigns will be undertaken with gammas, protons and electrons to investigate the device's performance following the expected end of life mission dose. A campaign using heavy ions is also planned to check the susceptibility of the device to single event effects.

3. EXPERIMENTAL SETUP

3.1 Driving the CMOS sensor

To obtain performance measurements of the CIS107 and CIS115, the sensors are being operated using a Scientific Imaging System camera drive unit by XCAM Ltd. (Northampton, UK) [6]. The camera drive unit interfaces with a PC using Camera Link and has power and fibre optic connections to a PCB stack. The sensor is held in a Zero-Insertion Force (ZIF) socket, and supply voltages and clocks are generated according to the optically transmitted control signals (Figure 5). The sensor analogue outputs are buffered, correlated double sampling is carried out by differencing the signal and reset outputs and the resulting signal level is converted to the digital domain and communicated back to the control computer (Figure 4).

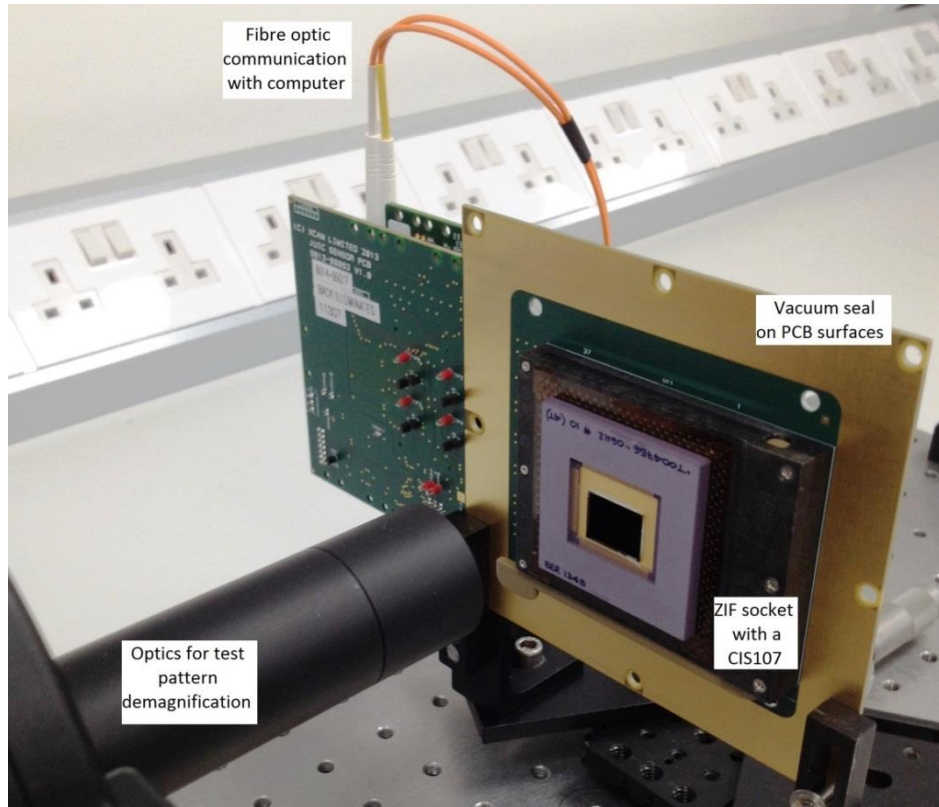


Figure 5. A ZIF socket is used to connect the devices to a PCB stack for testing. An optics setup (foreground) allows demagnification and focusing of test patterns held in a filter wheel onto the detector for testing. A single computer is used to control the motorized optic components and camera drive system.

3.2 Optical test bench

For optical characterisation, a test bench is being commissioned that allows automated focus and 2D scanning of slits, spots, flat fields or test patterns onto the detector. The focusing and scanning is achieved using three orthogonally arranged translational stages on which a computer controlled filter wheel holding the set of masks is mounted. A light source illuminates the mask and which is de-magnified using either a lens pair or a microscope objective. For cryogenic testing, the sensor can be located within a vacuum chamber that includes a 4 mm thick N-BK7 window. Cooling can be provided using a Polycold PCC Compact Cooler (Cryotiger) which is in contact with the detector package via a thermal braid and cold finger, allowing the detector to be tested at temperatures down to below -100°C .

4. INITIAL CHARACTERISATION RESULTS

4.1 Responsivity measurement

The first CIS115 sensors to become available for preliminary testing are front-illuminated (Figure 1). A responsivity measurement was obtained by recording images whilst the sensor was exposed to an iron-55 source in a dark box, at room temperature. The energy spectrum has been obtained by differencing consecutive frames, removing any contribution from fixed pattern offset noise, but reducing the spectral resolution in this case. The absolute signal levels are plotted in Figure 6, on an energy scale in units of eV that has been calibrated using the K_{α} emission feature (5898 eV). Factoring the subsequent readout chain, the average output responsivity for the CIS115 is $48.3 \mu\text{V electron}^{-1}$. The responsivity is greater than the measurement obtained in the relevant CIS107 pixel and output type ($35 \mu\text{V electron}^{-1}$), which is expected following the design modifications.

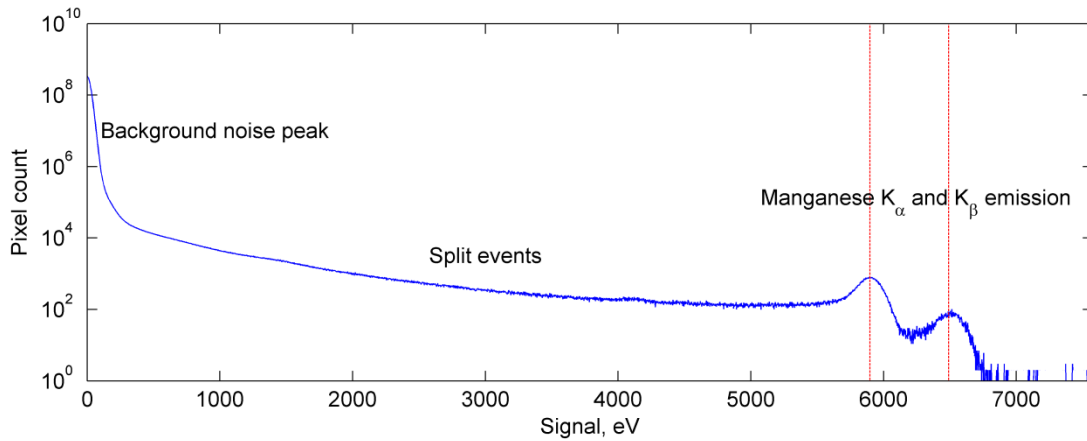


Figure 6. Iron-55 source spectrum, as recorded with a front illuminated CIS115 at room temperature. The K_{α} and K_{β} manganese emission lines are clearly visible at 5898 eV and 6490 eV respectively, allowing the responsivity to be measured as $48.3 \mu\text{V electron}^{-1}$.

4.2 Readout noise

Images can be recorded containing negligible signal by operating the detector so that the photodiodes are reset immediately before readout (Section 2.2). A back-illuminated CIS107 and a front-illuminated CIS115 were operated in this mode to capture 100 images with a pixel sampling rate of 5 MHz per output. The pixel by pixel readout noise for output 2 has been determined and shows no spatial correlation, therefore only the readout noise spectrum is reproduced here (Figure 7). The measurement is not limited by contribution from the off-chip readout chain (equivalent to 1.2 electrons rms and 1.7 electrons rms for the CIS115 and CIS107 respectively). The mean readout noise measured for the CIS115 is 4.25 electrons rms, which is significantly better than the CIS107 performance (5.6 electrons rms) and explained by the design modifications made.

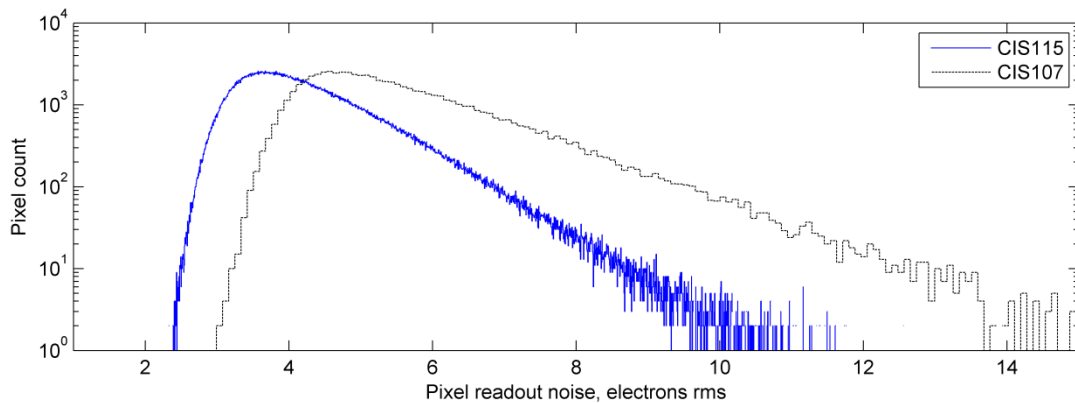


Figure 7. The pixel by pixel readout noise performance characterised for output 2 from the relevant pixel variant from the CIS107 and a CIS115 sensor. The CIS115 has a better noise performance due to design modifications. The histogram bin width used here is wider for the CIS107 due to the number of pixels suitable for comparison being smaller.

4.3 Dark current

To obtain a dark current measurement, the detector was placed in a dark box and further shielded from stray light. A series of images were recorded using integration times from 0 seconds to 300 seconds, with the device at room

temperature ($23 \pm 2^\circ\text{C}$). After removal of the pixel by pixel offset, the digital number signal values are converted to electrons using the calibration obtained from the iron-55 spectrum (uniform pixel responsivity is assumed). The dark signal generation was calculated on a pixel by pixel basis using the integration time where the signal level was approximately 1616 electrons, where the iron-55 responsivity measurement is valid. A map of the dark signal generation for a region of interest from the centre of the device is shown in Figure 8 and converted to a dark current per pixel spectrum is shown in Figure 9.

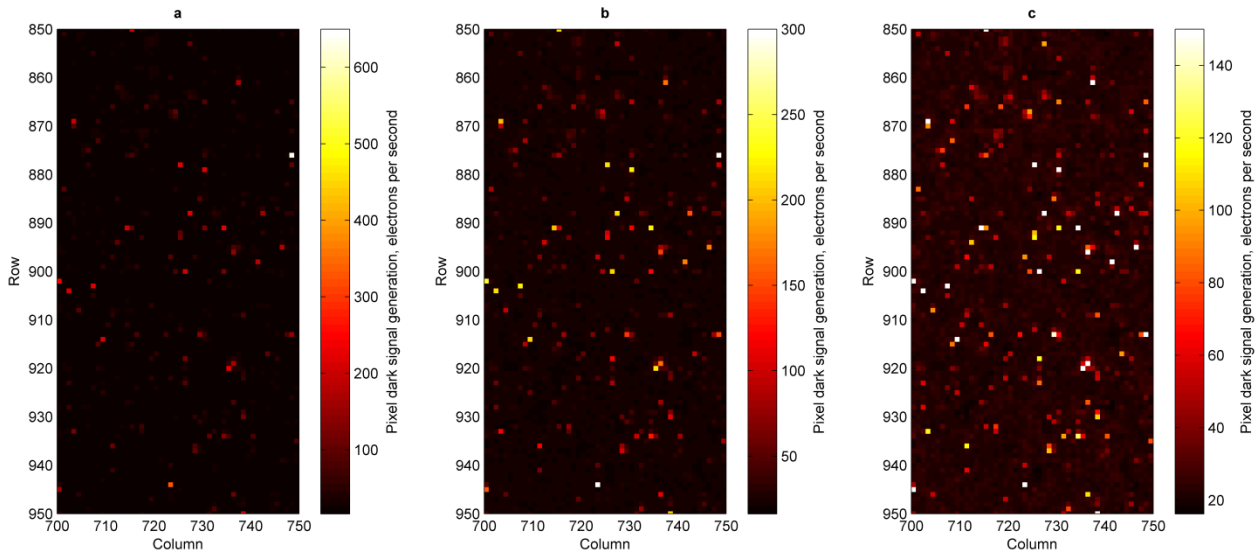


Figure 8. The dark signal generation for a region of interest from the centre of a CIS115’s imaging area (serial number 14901-25-32E) is shown here for three different color scales. The majority of pixels have a low level of dark current, at approximately 22 electrons per second. Isolated pixels and clusters of pixels are also present with higher levels of dark current generation.

The majority of pixels have dark signal generation rates close to the median level of $22.2 \text{ electrons second}^{-1} \text{ pixel}^{-1}$; however 5.6% of pixels have been measured with greater than 30 electrons per pixel. These ‘bright pixels’ contribute to a tail in the dark signal generation spectrum with notable features, such as the peak with a dark signal generation of approximately 220 electrons per second. Further work is required to investigate the cause of these features. During typical operation in JANUS, the CIS115 will be approximately 70°C colder and use integration times shorter than 100 ms, which will suppress the contribution of the dark signal to the noise background. However, future test campaigns will be used to investigate radiation-induced damage that is expected to increase the average dark signal generation and frequency of bright pixels [7].

4.4 Scan of optical spot along row of CIS107

Front illuminated devices are known to have reduced quantum efficiencies and variations in light response across a pixel due to the absorption of photons in the non-sensitive electrical layers of the device. However, back-illuminated devices suffer much less from this problem due to only a thin and spatially uniform region of the surface being non-sensitive to light. To investigate if a significant level of variation in light response was still present in back-illuminated device, a 640 nm LED was used to illuminate a $5\mu\text{m}$ pinhole. The spot was focused and demagnified onto a back-illuminated CIS107 using a microscope objective and scanned in steps across the columns (x dimension) and along the centre of a row.

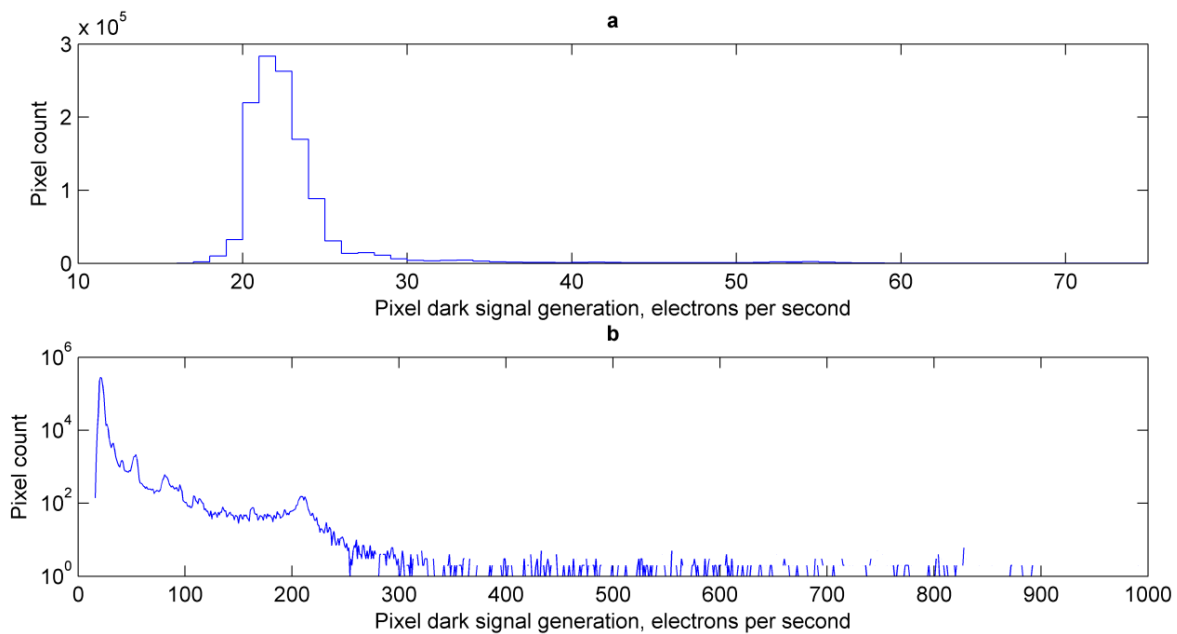


Figure 9. Dark signal generation per pixel for the central imaging area of the CIS115 at room temperature shows the majority of pixels generate approximately 22 electrons per second. A tail of pixels with higher dark current values is observed but further work is required to explain the features in the tail.

During the scan, the vertical position in the row (y) was maintained to be central in the row, compensating for any angle between the direction of translational stage movement and the sensor's rows. The positions of the scan are shown in Figure 10a. The total signal in the spot was averaged from 100 images, using both a 3×3 and a 5×5 pixel area, centred on the pixel with the maximum signal (Figure 10b). The variation across each pixel is small at approximately 2%, but step changes are observed as the centre of the focused spot crosses the boundary from one pixel to the next. The penetration depth of the 640 nm photons is approximately $7.5 \mu\text{m}$ (c.f. $\sim 10 \mu\text{m}$ back-thinned silicon), therefore a high proportion of photons are expected to penetrate close to the front surface of the detector to the regions containing the pixel electronics. Further characterisation is planned to contrast the performance of front and back-illuminated sensors at different illumination wavelengths.

5. CONCLUSIONS AND FUTURE WORK

A test bench to operate and characterise the sensor for the high resolution camera, JANUS, is being constructed and commissioned. A single back-illuminated CIS115 has been baselined for the focal plane of the camera, recording 1.5 MPixel images that will be used to map the surfaces of the icy moons, study the weather of Jupiter's atmosphere, and image other bodies of the Jovian system. Whilst the first CIS115s were being manufactured, a sensor characterisation test bench and camera has been commissioned using the precursor sensor, the CIS107. The first CIS115s to be manufactured have been front-illuminated, and preliminary characterisation tests have shed first light on the expected performance levels of the back-illuminated CIS115.

Average output responsivity of a front-illuminated CIS115 since been measured using an iron-55 radiation source to be $48.3 \mu\text{V}/\text{electron}$. The pixel by pixel readout noise spectrum is shown in Figure 7, with a mean readout noise value of 4.25 electrons rms. When uniform responsivity is assumed, the majority of pixels have a dark current of $22.2 \text{ electrons s}^{-1}$ (7.2 pA cm^{-2}) at room temperature ($23 \pm 2^\circ\text{C}$), whilst 5.6% of pixels exhibit dark signal generation greater than $30 \text{ electrons s}^{-1}$.

Further characterisation of the sensor will include a signal-dependent responsivity mapping on a pixel-by-pixel basis. Test procedures to measure properties such as full well capacity, dark signal generation as a function of temperature,

image lag, quantum efficiency and spatial resolution (through MTF, line or spot techniques) will also be developed in the near future.

The Jovian environment is particularly hostile with a high fluence of energetic charged particles being trapped in the magnetic field. Radiation campaigns to investigate the performance of the CIS115 following exposure to protons, gammas, heavy ions and electrons will be undertaken shortly to validate its expected end of life performance.

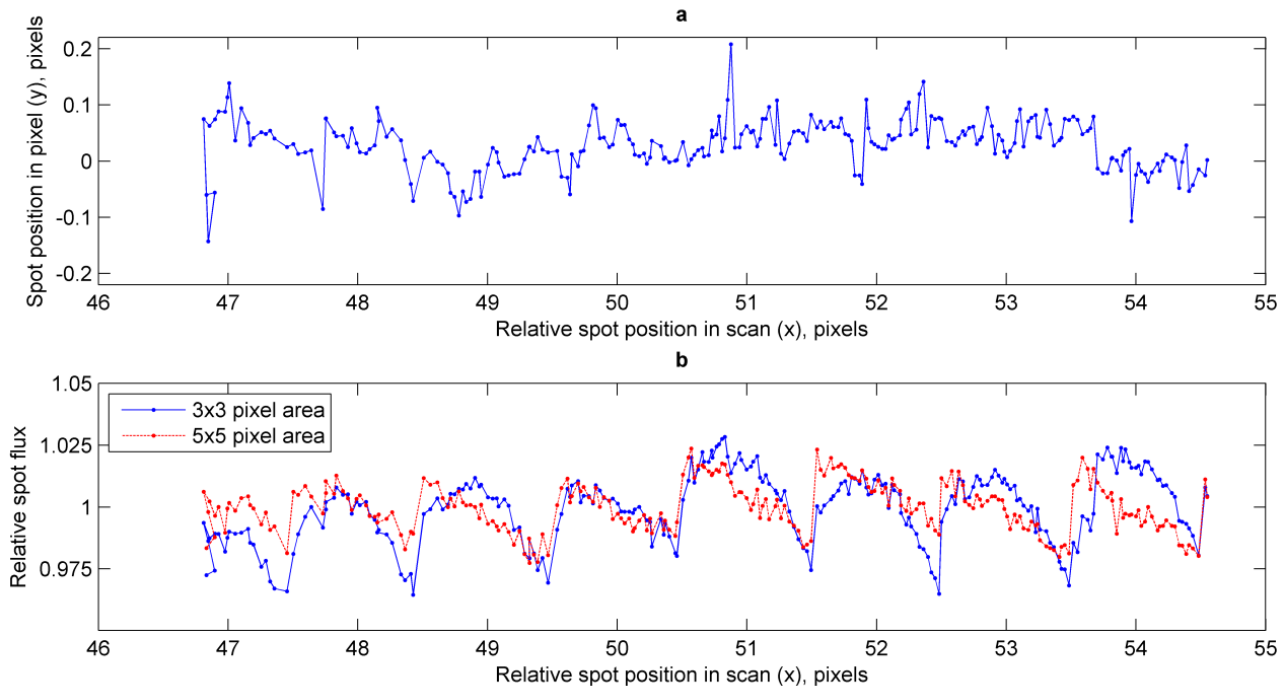


Figure 10. (a) The spot was scanned across the device parallel to the row direction, and maintained in the centre of the row. (b) Total signal in the spot, calculated by summing the signal from the pixels surrounding the one with maximum signal.

ACKNOWLEDGEMENTS

The CIS107 was designed by e2v and part-funded by Airbus Defence & Space (formerly Astrium) and CNES.

REFERENCES

- [1] Grasset, O., Dougherty, M.K., Coustenis, A., Bunce, E.J., Erd, C., Titov, D., Blanc, M., Coates, A., Drossart, P., Fletcher, L.N., Hussmann, H., Jaumann, R., Krupp, N., Lebreton, J.-P., Prieto-Ballesteros, O., Tortora, P., Tosi, F., Van Hoolst, T., "JUper ICy moons Explorer (JUICE): An ESA mission to orbit Ganymede and to characterise the Jupiter system," *Planetary and Space Science* 78, 1-21 (2013).
- [2] ESA, "JUICE Assessment Study Report (Yellow Book)", ESA/SRE, 13 January 2012, <http://sci.esa.int/juice/49837-juice-assessment-study-report-yellow-book/#>, (2 July 2014).
- [3] Jaumann, R., Palumbo, P., Hoffmann, H., Cremonese, G., Lara, L., Della Corte, V., Schmitz, N., Debei, S., Michaelis, H., Lichopoj, A., Magrin, D., Mazzotta Epifanti, E., Mottola, S., Ragazzoni, R., Zusi, M., Holland, A., "JANUS on the JUICE Mission: the Camera to Investigate Ganymede, Europa, Callisto and the Jovian System," *EPSC2013-506* 8, 1-2 (2013).

- [4] Dohlen, K., Saisse, M., Claeysen, G., Lamy, P., Boit, J.-L., "Optical designs for the Rosetta narrow-angle camera," *Optical Engineering* 35(4), 1150-1157 (1996).
- [5] e2v technologies plc., "CIS115 Back-Side Illuminated (BSI) CMOS Image Sensor Datasheet," A1A-778715 Version 1, private communication, February 2014.
- [6] XCAM Ltd., 10 September 2012, www.xcam.co.uk (6 June 2014).
- [7] Dryer, B., Holland, A.D., Murray, N.J., Jerram, P., Robbins, M., Burt, D., "Gamma radiation damage study of 0.18 μm process CMOS image sensors," *Proc. SPIE* 7742, 77420E (2010).